Nature of Prominences and their role in Space Weather
Proceedings IAU Symposium No. 300, 2013
B. Schmieder, J.-M. Malherbe & S. T. Wu, eds.

doi:10.1017/S1743921313011009

FIP bias in a sigmoidal active region

D. Baker[1], D. H. Brooks[2], P. Démoulin[3], Lidia van Driel-Gesztelyi[1,3,4], L. M. Green[1], K. Steed[5], J. Carlyle[1]

[1]University College London, Mullard Space Science Laboratory, Holmbury St Mary, Dorking, Surrey, RH5 6NT, UK
email: deborah.baker@ucl.ac.uk

[2]College of Science, George Mason University, 4400 University Drive, Fairfax, VA 22030, U.S.A.

[3]LESIA, Observatoire de Paris, CNRS, UPMC Université Paris-Diderot, 92195, Meudon, France

[4]Konkoly Observatory, Research Centre for Astronomy and Earth Sciences, Hungarian Academy of Sciences, PO Box 67, 1525, Budapest, Hungary

[5]Centre for Mathematical Plasma Astrophysics, KU Leuven, Celestijnenlaan 200B, 3001 Leuven, Belgium

Abstract. We investigate first ionization potential (FIP) bias levels in an anemone active region (AR) - coronal hole (CH) complex using an abundance map derived from *Hinode*/EIS spectra. The detailed, spatially resolved abundance map has a large field of view covering $359'' \times 485''$. Plasma with high FIP bias, or coronal abundances, is concentrated at the footpoints of the AR loops whereas the surrounding CH has a low FIP bias, ∼1, i.e. photospheric abundances. A channel of low FIP bias is located along the AR's main polarity inversion line containing a filament where ongoing flux cancellation is observed, indicating a bald patch magnetic topology characteristic of a sigmoid/flux rope configuration.

Keywords. Sun: abundances, Sun: active region, Sun: coronal hole, solar wind.

1. Introduction

Elemental abundances and their variations in space and time are all-important to our understanding of the physical processes fundamental to space weather. Seemingly, the most abundant elements of the Sun can be divided into two distinct groups according to their first ionization potential (FIP): low-FIP (<10 eV) and high-FIP (>10 eV) elements. In the corona, low-FIP elements are enhanced over photospheric abundance levels by a factor of 3–4, in contrast with high-FIP elements which maintain the elemental distribution of the photosphere. It is convenient to express the so-called FIP effect in terms of FIP bias, which is the ratio of the elemental abundance in the corona to the elemental abundance in the photosphere.

Plasma with photospheric abundances can be found in erupting prominences (Widing *et al.* 1986), newly emerging active regions (ARs; Sheeley 1995, 1996; Widing 1997), and in coronal holes (CHs; Brooks & Warren 2011; Feldman *et al.* 1998; Feldman & Widing 1993). Observational studies indicate that coronal abundances vary substantially from structure to structure and with time. FIP bias levels in established ARs are ∼4–6 and increase to 8–16 in older ARs (Feldman & Widing 2003; Widing & Feldman 1995). In situ measurements of the solar wind (SW) have established that low-FIP elements are enhanced by a factor of 3–4 in the slow wind, comparable to FIP bias levels observed in ARs, whereas composition of the fast wind is ∼1, similar to levels found in CHs (Gloeckler

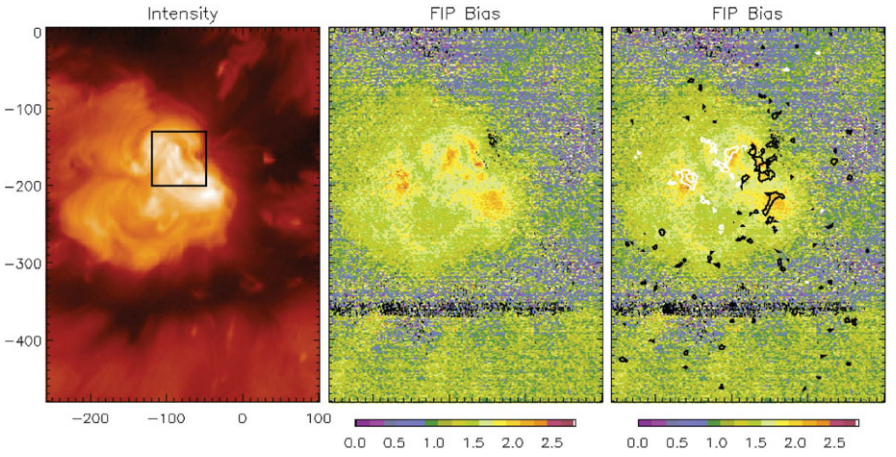

Figure 1. *Hinode*/EIS maps at 02:47 UT on October 17, 2007. Left: Fe XII 195.119 Å intensity map. The black box shows the field of view of Figure 2. Middle and right: S X 264.223 Å – Si X 258.375 Å abundance map (middle) overplotted with SOHO/MDI contours of ±100 G (right).

& Geiss 1989). Hence, elemental abundances have been used to connect SW plasmas to their source regions.

2. Observations

A small AR was observed inside an on-disk CH on October 17, 2007. During emergence of the bipole inside the CH, the AR interacts with the surrounding CH field and its magnetic connectivities get reorganized by way of interchange reconnection. As a result, new loops extend radially from the location of the included AR polarity, creating the characteristic anemone AR configuration. At the time of the *Hinode*/EIS raster, a filament is present in the AR along the main polarity inversion line (PIL). By 18:00 UT on the 17th, a sigmoid/flux rope is forming via flux cancellation. This mechanism was proposed by van Ballegooijen & Martens (1989). Finally, a coronal mass ejection (CME) erupts at approximately 07:30 UT on the 18th. The *Hinode*/EIS Fe XII 195.119 Å intensity map (left panel) and S X 264.223 Å – Si X 258.375 Å (middle and right panels) abundance map are shown in Figure 1. See Baker *et al.* (2012) for a complete account of the AR-CH complex observations and Baker *et al.* (2013) for a description of the method used to construct the abundance map derived from *Hinode*/EIS spectra.

3. Results

Large-scale structures are evident in the abundance map (middle panel of Figure 1). The composition of the CH surrounding the AR is photospheric with a FIP bias of ∼1. Levels in the anemone AR range between ∼2 and 3. Although the general FIP bias in the AR is somewhat low compared with previous compositional studies of ARs (e.g. Widing & Feldman 1995), it is clearly above the level of FIP bias in the CH, therefore, the AR has a coronal composition.

Detailed structure is discernible within the AR. Patches of high-FIP bias are located close to concentrations of relatively strong magnetic flux density at AR loop footpoints. Figure 1, right panel, shows the abundance map overplotted with SOHO/MDI contours of ±100 G. The contours are cospatial with areas of high-FIP bias. Furthermore, pathways

https://doi.org/10.1017/S1743921313011009 Published online by Cambridge University Press

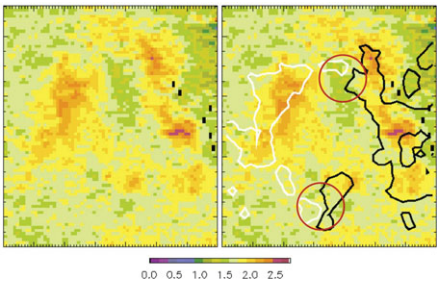

Figure 2. Left: Zoomed abundance map showing the sigmoid region indicated by the black box in the left panel of Figure 1. Right: Zoomed abundance map overplotted with SOHO/MDI contours of ±100 G. Red circles indicate locations of principal flux cancellation along the main PIL.

of slightly enhanced FIP bias (∼2–2.5) appear to trace loops connecting opposite polarity magnetic flux within the AR.

In Figure 2 (left panel), the abundance map is zoomed to highlight the sigmoid region within the box overplotted on the *Hinode*/EIS Fe XII 195.119 Å intensity map in Figure 1. The zoomed map shows an inverse S-channel of low-FIP bias along the main PIL which hosts a filament within the AR where a sigmoid/flux rope is forming and will erupt soon thereafter (Baker *et al.* 2012). The two principal sites of flux cancellation along the PIL, indicated by the red circles in Figure 2, are located in low-FIP bias areas.

4. Discussion

FIP bias in established ARs can reach values significantly greater than 4 which is higher than the levels of 2–3 found in this anemone AR. Large variation in AR plasma composition is related to the variation in the average age of ARs (McKenzie & Feldman 1992; Widing & Feldman 2001). New flux emergence has photospheric composition (Sheeley 1995, 1996; Widing 1997; Widing & Feldman 2001), however, the FIP bias of evolving ARs progresses at approximately a constant rate toward coronal levels within days of emergence (Widing & Feldman 2001). In this case, the low level of FIP bias may be due to the fact that the anemone AR is mainly comprised of recently formed loops instead of the older loop structures of mature ARs (Young & Mason 1997). Although the AR is visible behind the eastern limb in STEREO/EUVI images one week prior to the *Hinode*/EIS observation, the AR's age should not be greater than ≈10 days as the average lifetime for such a small AR is measured in days (Schrijver & Zwaan 2008).

The low-FIP bias plasma of the surrounding CH may also contribute to the low levels in the AR. Since CH plasma undergoes very little modification upon emerging from the photosphere, its composition remains at levels close to 1, as was confirmed by this study. The anemone AR is entirely surrounded by low-FIP CH plasma which can readily mix with the high-FIP AR plasma via interchange reconnection. It is plausible that anemone ARs would have lower FIP bias levels compared with ARs surrounded by mixed magnetic polarities.

It is generally accepted that elemental fractionation takes place mainly in the chromosphere, where low-FIP elements are mostly ionized and high-FIP elements are partially neutral. Meyer (1996) and Widing & Feldman (2001) concluded that the footpoints and legs of loop-like structures are the likely sites for elemental fractionation and uplift to

https://doi.org/10.1017/S1743921313011009 Published online by Cambridge University Press

occur. We find strong evidence in support of their conclusions in the anemone AR. High-FIP bias is concentrated at the AR's loop footpoints close to where fractionation is believed to take place. In the young AR, there is insufficient time for high-FIP plasma to fill the coronal loops so we would expect to observe a concentration of high-FIP bias at the footpoints combined with the start of plasma mixing in some of the coronal loops. Loop traces of slightly enhanced FIP bias is suggestive of partial plasma mixing within AR loops.

Finally, the sigmoidal filament channel of low-FIP bias in Figure 2 is atypical of the global pattern of the AR FIP bias. We propose that this channel could be field lines in a flux rope formed by flux cancellation along the main PIL. This is highly suggestive of a bald patch (BP) topology where field lines are tangent to the photosphere. Converging/shearing motions induce the formation of a current sheet along the BP separatrix (Aulanier *et al.* 2010). Reconnection is expected to take place low down along the separatrix, lifting up photospheric plasma in the magnetic dips, implying a low-FIP bias when mixed with the coronal plasma of the reconnecting loops. *Hinode*/EIS abundance maps have a potential role to play in space weather forecasting by enhancing our ability to identify the early formation of flux ropes, which are possible sites of CMEs.

Acknowledgements

Hinode is a Japanese mission developed and launched by ISAS/JAXA, collaborating with NAOJ as a domestic partner, NASA and STFC (UK) as international partners. It is operated by these agencies in co-operation with ESA and NSC (Norway). LvDG and KS acknowledge the European Community FP7/2007-2013 programme through the eHEROES Network (EU FP7 Space Science Project Nos. 284461). KS also acknowledges the SWIFF Network (EU FP7 Space Science Project No. 263340). LvDG acknowledges the Hungarian government for grant OTKA K-081421. The work of DHB was performed under contract with the Naval Research Laboratory and was funded by the NASA Hinode program. JC thanks UCL and the Max Planck Institute for an Impact Studentship award. DB's work was supported by STFC.

References

Aulanier, G., Török, T., Démoulin, P., & DeLuca, E. E. 2010, *ApJ*, 708, 314

Baker, D., van Driel-Gesztelyi, L., & Green, L. M. 2012, *Solar Phys.*, 276, 219

Baker, D., Brooks, D. H., Démoulin, P., van Driel-Gesztelyi, L., Green, L. M., Steed, K., & Carlyle, J. 2013, *ApJ*, 778, 69B

Brooks, D. H. & Warren, H. P. 2011, *ApJ* (Letters), 727, L13

Feldman, U., Schühle, U., Widing, K. G., & Laming, J. M. 1998, *ApJ*, 505, 999

Feldman, U. & Widing, K. G. 1993, *ApJ*, 414, 381

—. 2003, *Space Sci. Revs*, 107, 665

Gloeckler, G. & Geiss, J. 1989, in American Institute of Physics Conference Series, Vol. 183, Cosmic Abundances of Matter, ed. C. J. Waddington, 49

McKenzie, D. L. & Feldman, U. 1992, *ApJ*, 389, 764

Meyer, J.-P. 1996, in Astronomical Society of the Pacific Conference Series, Vol. 89, Coronal Abundances, ed. Holt, S. S. and Sonneborn, G., 127

Schrijver, C. J. & Zwaan, C. 2008, Solar and Stellar Magnetic Activity (Cambridge, UK: Cambridge University Press)

Sheeley, Jr., N. R. 1995, *ApJ*, 440, 884

—. 1996, *ApJ*, 469, 423

van Ballegooijen, A. A. & Martens, P. C. H.. 1989, *ApJ*, 343, 971V

Widing, K. G. 1997, *ApJ*, 480, 400
Widing, K. G. & Feldman, U. 1995, *ApJ*, 442, 446
—. 2001, *ApJ*, 555, 426
Widing, K. G., Feldman, U., & Bhatia, A. K. 1986, *ApJ*, 308, 982
Young, P. R. & Mason, H. E. 1997, *Solar Phys.*, 175, 523

https://doi.org/10.1017/S1743921313011009 Published online by Cambridge University Press